

Can a form of electrode/electrolyte interface change the ranges of dynamic instabilities?

O.I. Gichan^{1*}, V.V. Pototskaya²

¹Chuiko Institute of Surface Chemistry of National Academy of Sciences of Ukraine, 17 Henerala Naumova Str., Kiev 03164, Ukraine

²Vernadskii Institute of General & Inorganic Chemistry of National Academy of Sciences of Ukraine, 32-34 Palladina Prosp., Kiev 03142, Ukraine

Received September, 24, 2014; Revised February, 4 2015

Based on the theory of electrochemical impedance spectroscopy the ranges of dynamic instabilities leading to oscillatory and bistable behaviour in a model electrocatalytic process with a preceding chemical reaction in the Nernst diffusion layer and the potential-dependent adsorption/desorption of electroactive species under potentiostatic conditions were compared for a case of spherical, cylindrical and planar electrode.

Keywords: Electrochemical impedance spectroscopy, Electrode geometry, Electrocatalytic mechanism, Oscillations, Bistability

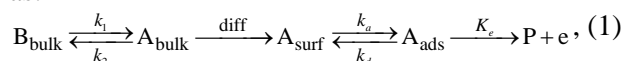
INTRODUCTION

The frequent appearance of oscillations and pattern formation at electrolyte/electrode interface can be explained by the inherently nonlinear electrochemical kinetics and far from equilibrium performance of electrochemical experiments [1-14]. In impedance spectroscopy [15, 16], bifurcations leading to oscillatory and bistable dynamics can be represented by zero of impedance or admittance [9-14]. By instabilities, or bifurcations, we mean a qualitative change in the dynamical states of a system, occurring with the attainment of a certain critical, bifurcation value of the control parameter.

In the paper, we will answer the question whether a simple change in a form of electrode/electrolyte interface at fixed values of other parameters of the electrochemical system can influence its dynamic behaviour. In a model process, the electroactive species of one sort are produced by a preceding chemical reaction, diffuse from the Nernst diffusion layer to the electrode surface, where they are adsorbed and electrochemically oxidized. We consider in detail derivation of necessary conditions for the Hopf and saddle-node instabilities in this electrocatalytic process on a surface of cylindrical electrode and compare these results with those obtained for the planar and spherical ones [5-8].

THEORY

The scheme of the model process can be written as:



where k_1 , k_2 are the rate constants of chemical reaction in the bulk solution, k_a , k_d , K_e are the rate constants of adsorption, desorption and electron transfer. The last step of the reaction is considered to be irreversible.

Neglecting the ohmic losses and double layer influence, the main kinetic equations are:

$$\frac{\partial c(r,t)}{\partial t} = D \frac{1}{r} \frac{\partial}{\partial r} \left(r \frac{\partial c(r,t)}{\partial r} \right) - kc(r,t), \quad (2)$$

$$\Gamma \frac{d\theta}{dt} = v_1(t) - v_2(t, E(t)). \quad (3)$$

Here, $c(r, t)$ is the electroactive species A concentration, $c(r, t) = c_0 + u$ (u is the concentration deviation from the equilibrium value c_0 coinciding with the bulk concentration of species), t – time, r – distance from the origin of coordinates which coincides with the center of the cylinder, $k = k_1 + k_2$ is the effective rate of a preceding homogeneous chemical reaction, $\theta(t)$ is the electrode surface coverage by the adsorbate, Γ is the maximum surface concentration at $\theta=1$, $v_1(t)$ and $v_2(t)$ – the adsorption-desorption rate and the electron transfer rate, that satisfy the equations

$$v_1(t) = \Gamma k_a \exp(\gamma\theta(t)/2) c(r_0, t) (1 - \theta(t)) - \Gamma k_d \exp(-\gamma\theta(t)/2) \theta(t), \quad (4)$$

$$v_2(t) = \Gamma K_e(t) \theta(t) = \Gamma k_e \exp(\alpha b E(t)) \theta(t), \quad (5)$$

* To whom all correspondence should be sent:
E-mail: gichan@meta.ua

where r_0 is the electrode radius, α is the symmetry factor of electron transfer in the direction of oxidation, E is the electrode potential, k_e is the rate constant of electron transfer at $E(t)=0$, $b = F/(RT)$, F is the Faraday's number, R is the gas constant, T is the absolute temperature, γ is the attraction constant. Positive values of the attraction constant γ correspond to the attraction between adsorbed species, and its negative values correspond to the repulsion between adsorbed species. If attraction is small ($\gamma = 0$) the Frumkin isotherm passes in the Langmuir isotherm. Only positive value of the attraction constant leads to instability [9, 11].

As follows from eqn. (4), for the adsorption-desorption rate $\nu_1(t) = 0$, the adsorption-desorption of species A on the electrode surface under steady-state conditions is described by the Frumkin isotherm.

The boundary conditions allow for the fact that at the electrode surface diffusion flux is equal to the adsorption-desorption rate, and at the distance that exceeds δ the bulk concentration of species A is constant and equal to c_0

$$J_c(r_0, t) = -D \frac{\partial c(r, t)}{\partial r} \Big|_{r=r_0} = -\nu_1(t), \quad (6)$$

$$c(\delta, t) = c_0. \quad (7)$$

Here J_c is the diffusion flux, D is the diffusion coefficient, $\delta = r_0 + d$, d is the Nernst diffusion layer thickness.

In eqn. (2), we take into account the variation of the concentration only in the radius line. The dependence on the z and φ coordinates is absent.

The faradaic current density was determined according to the following equation

$$j_f(t) = F\nu_2(t) = F\Gamma k_e \exp[\alpha b E(t)] \theta(t). \quad (8)$$

Steady-State Conditions

Under steady-state conditions, i.e. when $d\theta/dt = 0$, $\partial c(r, t)/\partial t = 0$, from eqns. (2, 3) with boundary conditions (6, 7) one can obtain the steady-state concentration at the electrode surface $c_{st}(r = r_0)$, the steady-state electrode potential E_{st} and steady-state faradaic current density j_{fst}

$$c_{st}(r_0) = \frac{m_c c_0 + \Gamma k_d \theta_{st} \Omega_0 e^{-\gamma \theta_{st}/2}}{m_c + (1 - \theta_{st}) \Omega_0 \Gamma k_d e^{\gamma \theta_{st}/2}}, \quad (9)$$

$$E_{st} = (\alpha b)^{-1} \ln \left[\frac{m_c (c_0 - c_{st}(r_0))}{\Gamma k_e \theta_{st} \Omega_0} \right], \quad (10)$$

$$j_{fst} = \frac{F m_c (c_0 - c_{st}(r_0))}{\Omega_0}. \quad (11)$$

Here $m_c = D/d$, $\lambda = \sqrt{k/D}$,

$$\Omega_0 = \frac{1}{\lambda d} \left(\frac{K_0(x_0) I_0(x_\delta) - K_0(x_\delta) I_0(x_0)}{I_0(x_\delta) K_1(x_0) + I_1(x_0) K_0(x_\delta)} \right),$$

$$x_0 = r_0 \sqrt{k/D}, \quad x_\delta = (r_0 + d) \sqrt{k/D},$$

$I_0(x)$, $K_0(x)$ are modified zero-order Bessel functions, $I_1(x)$, $K_1(x)$ are first-order modified Bessel functions of first and second kind, respectively.

The potential is counted off from the zero-charge potential of the electrode free from species.

Impedance Spectra and System Dynamic Instabilities

Under potentiostatic experimental conditions, the studies of linear stability of the electrochemical system near the steady state are based on analysis of variation of the impedance zero values under variation of the electrode potential [9-14]. A *Hopf bifurcation* can be realized in the system when its complex impedance is equal to zero at nonzero frequency, $Z(\omega) = 0$ at $\omega = \omega_H \neq 0$ ($\omega = 2\pi f$, f – frequency). At Hopf bifurcation point the system can produce its own undamped periodic oscillations with frequency ω_H , so in the case of influence on the system of an external signal with a frequency exactly coinciding with this value, the external signal will pass through the system without resistance [11].

A *saddle-node bifurcation* can appear when $Z(\omega) = 0$ at $\omega = 0$, i.e. in points where polarization resistance of an electrochemical system $Z_P = \lim_{\omega \rightarrow 0} Z_f(\omega)$ is equal to zero [9-11]. This bifurcation initiates in a non-equilibrium system bistability – the coexistence of two stable steady states at the same values of the parameters. Which one is chosen depends on where the system comes from, i.e. on initial conditions. In this sense the bistable system has a memory. The saddle – node bifurcations always come in pairs and lead to hysteresis.

Calculation of Faradaic Impedance

To calculate faradaic impedance of the system, its behavior was analyzed under a low periodical signal $\Delta E(t) = \Delta E_0 e^{i\omega t}$ applied in a given point of the steady-state voltammetric curve

$$E(t) = E_{st} + \Delta E_0 e^{i\omega t}, \quad (12)$$

where $i = \sqrt{-1}$, ΔE_0 is the amplitude of a low periodical signal.

In response to this excitation, the electrode surface coverage $\theta(t)$, faradaic current density $j_f(t)$, and surface concentration $c(r_0, t)$ will oscillate near the steady – state values, namely

$$\begin{aligned} \theta(t) &= \theta_{st} + \Delta\theta_0 e^{i\omega t}, \\ j_f(t) &= j_{fst} + \Delta j_f(E, \theta), \\ c(r_0, t) &= c_{st}(r_0) + \Delta c(r_0, \theta). \end{aligned} \quad (13)$$

The expression for faradaic impedance in the Laplace image space $\bar{F}(s) = \int_0^\infty f(t) e^{-st} dt$ as a function of complex frequency $s = \sigma + j\omega$ takes the form of

$$\bar{Z}(s) = \frac{\Delta \bar{E}(s)}{\Delta \bar{j}_f(s)}. \quad (14)$$

Omitting some mathematical computations, let us write the resultant expression for faradaic impedance in the Laplace image space

$$\bar{Z}_f(s) = R_{ct} \left\{ 1 + \frac{\partial \theta v_2 (1 + \Omega_s \partial_c v_1)}{\Gamma s (1 + \Omega_s \partial_c v_1) - \partial \theta v_1} \right\}, \quad (15)$$

where partial derivatives are designated here as $\partial_x u = \partial u / \partial x$ and the following notations are introduced:

$$\begin{aligned} \Omega_s &= \frac{1}{\lambda_s D} \left(\frac{K_0(x_{0s}) I_0(x_{\delta s}) - K_0(x_{\delta s}) I_0(x_{0s})}{I_0(x_{\delta s}) K_1(x_{0s}) + I_1(x_{0s}) K_0(x_{\delta s})} \right), \\ \partial \theta v_2 &= \Gamma k_e \exp(\alpha b E_{st}), \quad \lambda_s = \sqrt{(k+s)/D}, \\ x_{0s} &= r_0 \sqrt{(k+s)/D}, \quad x_{\delta s} = (r_0 + d) \sqrt{(k+s)/D}, \\ \partial \theta v_1 &= \Gamma \{ k_d \exp(-\gamma \theta_{st}/2) [\gamma \theta_{st}/2 - 1] + \\ &\quad + k_a \exp(\gamma \theta_{st}/2) c_{st}(r_0) [\gamma(1 - \theta_{st})/2 - 1] \}, \\ \partial_c v_1 &= \Gamma k_a (1 - \theta_{st}) \exp(\gamma \theta_{st}/2), \\ R_{ct} &= 1 / \frac{\partial i_{fst}}{\partial E_{st}} = 1 / F \Gamma \alpha b k_e \exp(\alpha b E_{st}) \theta_{st} \text{ is the} \end{aligned}$$

charge transfer resistance.

In our calculations we ignored the electrolyte resistance and the double-layer impedance. In this case, the impedance of the model system under consideration is equal to faradaic impedance, $Z = Z_f$.

Assuming that the double-layer charging and the faradaic process are not coupled and that the double-layer capacitance C_{dl} is associated in parallel with the faradaic impedance, the interfacial impedance is given by

$$Z_{int} = \left(\frac{1}{Z_f} + i\omega C_{dl} \right)^{-1}. \quad (16)$$

The impedance Z of the cell is the sum of the series resistance R_s and the interfacial impedance Z_{int}

$$Z = R_s + Z_{int}, \quad (17)$$

where R_s is the sum of the electrolyte and external resistance.

It is known that the effect of ohmic resistance on the impedance spectrum is reduced to a horizontal shift of impedance diagrams in the complex plane [10]. This can result in a change in the number of bifurcation points in the system.

It was shown that the parameter R_s can regulate the ranges of Hopf and saddle – node instabilities in an opposite way [7, 8]. Its increase results in a Hopf instability region decrease and a saddle – node instability region increase. There are threshold values of the parameter R_s critical for appearance and disappearance of the instabilities in question. The threshold values of the ohmic resistance depend on the preceding chemical reaction rate in bulk solution.

Double layer capacitance does not affect either Hopf or saddle-node bifurcation points. The effect of this parameter on the impedance spectrum is manifested only in the high–frequency region [7, 8].

Determination of Hopf Bifurcation Points

To determine the Hopf bifurcation points, impedance zero points were studied under electrode potential variation. The impedance zero points were found according to the following equation:

$$Z = R_s + Z_{int} = 0. \quad (18)$$

In order to satisfy condition (18), it is necessary that

$$\begin{cases} \text{Re}[Z] = 0 \\ \text{Im}[Z] = 0. \end{cases} \quad (19)$$

One can solve the system of equations only numerically.

Determination of Saddle-Node Bifurcation Points

To determine saddle – node bifurcation points, the solutions of the following equation were studied numerically:

$$Z_p + R_s = 0, \quad (20)$$

where polarization resistance of the electrochemical system is

$$Z_P = R_{ct} \left\{ 1 - \frac{\partial_{\theta} v_2 (1 + \Omega_0 \partial_c v_1)}{\partial_{\theta} v_1} \right\}. \quad (21)$$

In order to pass from the Laplace space to the Fourier space, it is necessary to perform a substitution $s = i\omega$.

In the model calculation, the following values of system parameters were assumed: $\Gamma = 10^{-9}$ mol/cm²; $\gamma = 8$; $\Gamma k_a = 0.1$ cm s⁻¹; $\Gamma k_d = 10^{-5}$ mol/cm² s; $k_e = 10$ s⁻¹; $D = 10^{-5}$ cm²/s; $\alpha = 0.5$; $d = 10^{-3}$ cm; $c_0 = 7.5 \cdot 10^{-6}$ mol/cm³; $r_0 = 10^{-4}$ cm (for spherical and cylindrical electrodes); $C_{dl} = 2.5 \cdot 10^{-5}$ F cm⁻²; $F = 96484$ C/mol; $T = 300$ K; $R = 8.314$ J/mol K; $b = F/(RT) = 38.7$ V⁻¹; $k = 10$ s⁻¹; $R_s = 0.3$ Ohm cm².

All numerical calculations were performed on the basis of the mathematical package Mathematica™.

RESULTS AND DISCUSSION

Fig. 1 schematically presents a cylindrical electrode of radius r_0 and the Nernst diffusion layer with thickness d , where concentration of electroactive species varies. At the distance that exceeds δ the bulk concentration of species is constant. The variation of the concentration is taken into account only in the radius line. The dependence on the z and φ coordinates is absent.

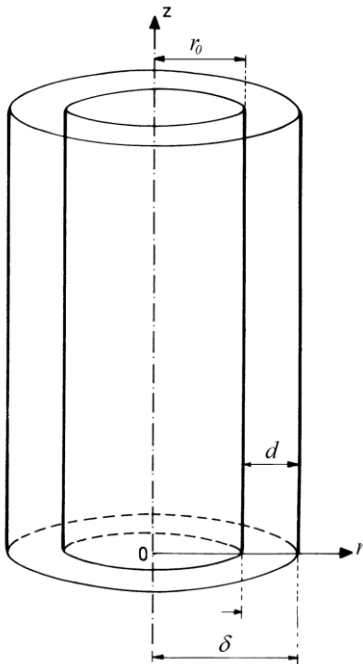


Fig. 1. Schematic presentation of cylindrical electrode of radius r_0 and Nernst diffusion layer of d value.

As shown by the performed calculations, the steady-state polarization j_{fct} , E_{st} - curves are N-shaped form with the negative differential resistance (NDR) region. Two opposite factors

determine the current value in the model process: the increase in the potential and the decrease in the concentration of electroactive species in the near-electrode layer due to the adsorption. The later depends on the potential in the non-linear fashion. When the diffusion rate of electroactive species is equal to the rates of processes occurring on the electrode, the voltammogram contains a maximum. If the rate of consumption of reacting species is predominant, the faradaic current decreases due to the insufficient rate of their delivery from diffusion layer, while the potential increases.

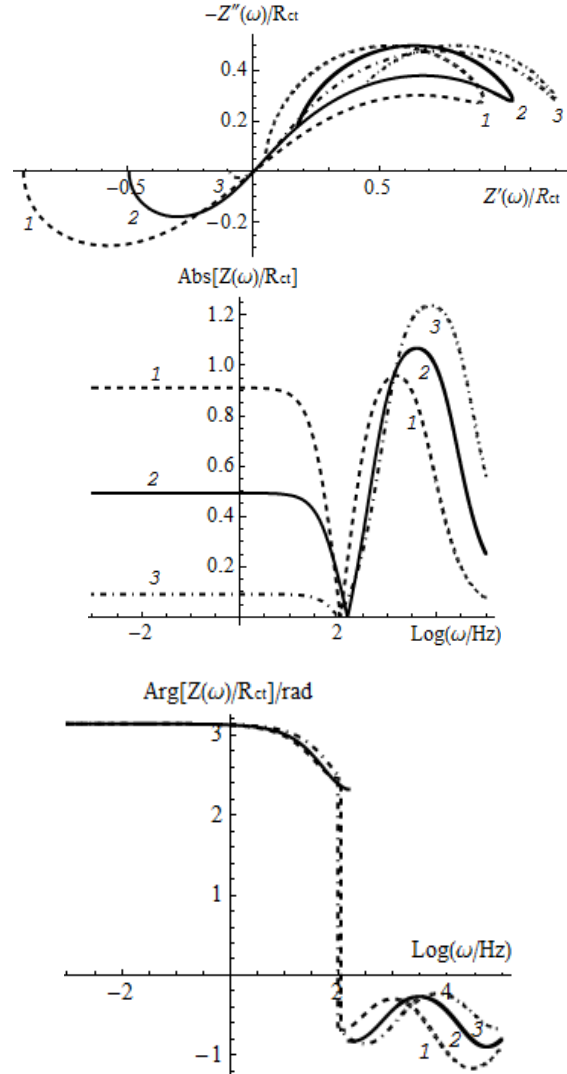


Fig. 2. (a) Nyquist diagrams of the behavior of total cell impedance normalized on charge transfer resistance in a complex plane at the Hopf bifurcation points (H_1) for the case of planar (1), cylindrical (2) and spherical (3) electrodes. Dependences of (b) absolute impedance and (c) impedance phase angle on $\log \omega$ at the bifurcation points.

This is the range of the NDR. The Hopf and saddle-node bifurcation points are in this region. The current density value is the smallest for the

case of a planar electrode; it is the largest for the case of a spherical electrode.

Figs. 2a–2c and Figs. 3a–3c show the Nyquist and Bode diagrams for total cell impedance calculated according to formula (16) in the Hopf (H_1) and saddle-node (SN_1) bifurcation points for a planar, cylindrical and spherical electrode (table).

Table 1. Parameter values of the electrochemical system at the bifurcation points.

Electrode form	Bifurcation point	ω/Hz	θ	$i_{fst}/\text{A cm}^{-2}$	E_{st}/V
plane	H_1	110	0.583	0.00760	0.13455
	SN_1	0	0.374	0.00545	0.14028
	SN_2	0	0.232	0.00330	0.13901
cylinder	H_1	152	0.565	0.02427	0.19618
	SN_1	0	0.442	0.02016	0.19927
	SN_2	0	0.214	0.00916	0.19606
sphere	H_1	97	0.567	0.05239	0.23575
	SN_1	0	0.544	0.05080	0.23629
	SN_2	0	0.198	0.01622	0.22953
	H_2	59	0.196	0.01605	0.22959

For chosen values of the system parameters there are two Hopf bifurcation points for all electrodes. Let's consider the behavior of impedance in a complex plane at the Hopf bifurcation points H_1 (Figs. 2a). At the low-frequency range in the Nyquist diagram, there is a loop with a negative real part of impedance that indicates the existence of instability in the system. This inductive loop decreases as symmetry of electrode increases, i.e. for a planar electrode this loop is the largest, for a spherical electrode it is the smallest. Such change in electrode form leads to a change in a form of conductive loop with positive real part of impedance. The absolute impedance, $Abs[Z(\omega)/R_{ct}]$, turns to zero in the Hopf

bifurcation point at $\omega=\omega_H$ (Figs. 2b, 2c). This bifurcation frequency is different for case of planar, cylindrical and spherical electrode. In the Hopf bifurcation point the functional dependence of the impedance phase angle $Arg[Z(\omega)/R_{ct}]$ on $\log \omega$ changes drastically.

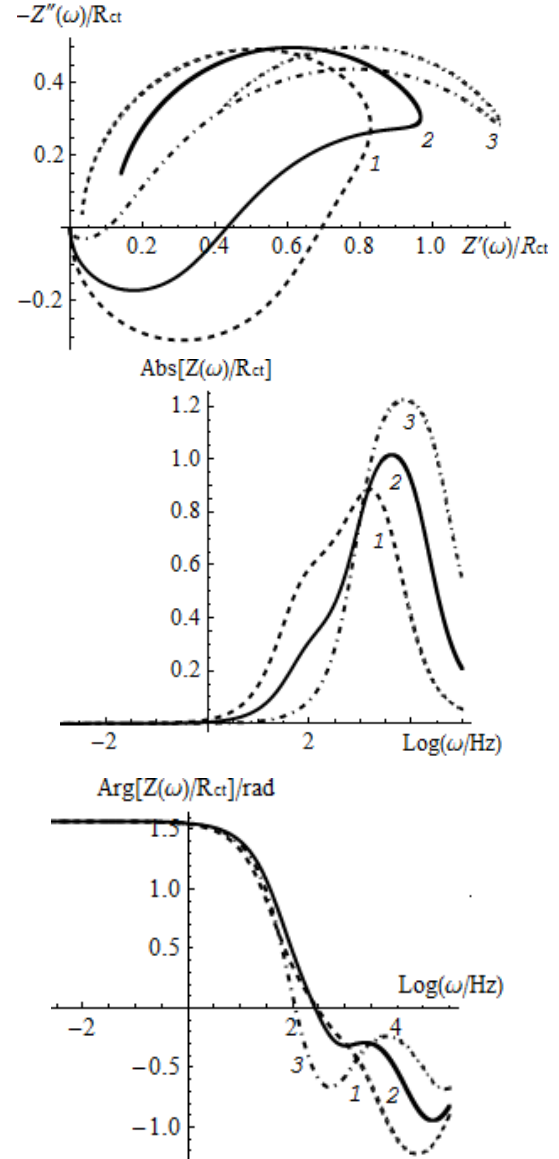


Fig. 3. (a) Nyquist diagrams of the behavior of total cell impedance normalized on charge transfer resistance in a complex plane at the saddle-node bifurcation points (SN_1) for the case of planar (1), cylindrical (2) and spherical (3) electrodes. Dependences of (b) absolute impedance and (c) impedance phase angle on $\log \omega$ at the bifurcation points.

The Nyquist diagrams in the saddle-node bifurcation points SN_1 are presented in Fig. 3a. An inductive loop with a positive real part of impedance increases as the symmetry of electrode decreases from spherical electrode to planar one. A conductive loop with a positive real part of impedance also changes. A decrease in the

symmetry of electrode results in a decrease in absolute impedance and change in its phase angle for bifurcation points under consideration.

CONCLUSIONS

Thus, we can conclude that a simple change in a form of electrode/electrolyte interface can change the dynamic stability of the model electrocatalytic process with a preceding homogeneous chemical reaction in the Nernst diffusion layer and the potential-dependent adsorption/desorption of electroactive species on the electrode surface under potentiostatic conditions. The analytically derived expression for total cell impedance allows us to investigate the possible realization of the Hopf and saddle-node instabilities in the electrochemical system in case of a spherical, cylindrical and planar electrode.

The region of bistability is wider for a spherical electrode than for a planar electrode. In contrast to this a decrease in the electrode symmetry is the reason for the Hopf instability region increase. Varying a form of electrode we can vary frequency of spontaneous current oscillations ω_H . This presents the way of possible control of dynamic behavior of real electrochemical systems.

REFERENCES

1. J. Eshkult, C. Ulrich, F. Björefors, L. Nyholm, *Electrochim. Acta*, **53**, 2188 (2008).
2. D. Sazou, M. Pavlidou, M. Pagitsas, *J. Electroanal. Chem.* **675**, 54 (2012).
3. Ts. Dobrovolska, D.A. López-Sauri, L. Veleva, I. Krastev, *Electrochim. Acta*, **79**, 162 (2012).
4. H. Okamoto, T. Gojuki, N. Okano, T. Kuge, M. Morita, A. Maruyama, Y. Mukouyama, *Electrochim. Acta*, **136**(1), 385 (2014).
5. V.V. Pototskaya and O.I. Gichan, *Russ. J. Electrochem.*, **47**(3), 336 (2011).
6. V.V. Pototskaya and O.I. Gichan, *Russ. J. Electrochem.*, **48**(2), 154 (2012).
7. O.I. Gichan and V.V. Pototskaya, *Electrochimica Acta*, **112**, 957 (2013).
8. V.V. Pototskaya and O.I. Gichan, *Russ. J. Electrochem.*, **50**(11), 1009 (2014).
9. M.T.M. Koper and J.H. Sluyters, *J. Electroanal. Chem.*, **371**, 149 (1994).
10. M.T.M. Koper, *Adv. Chem. Phys.*, **92**, 161 (1996).
11. M.T.M. Koper, *J. Chem. Soc. Faraday Trans.*, **94**, 1369 (1998).
12. M. Naito, N. Tanaka, H. Okamoto, *J. Chem. Phys.*, **111**, 9908 (1999).
13. A. Sadkowsky, *J. Electroanal. Chem.*, **485**, 119 (1999).
14. F. Berthier, J.P. Diard, C. Montella, *Electrochim. Acta*, **44**, 2397 (1999).
15. Z.B. Stoynov, B.M. Grafov, B. Savova-Stoynova, V.V. Elkin, *Elektrokhimicheski impedans (Electrochemical Impedance)*, Nauka, Moscow, 1991.
16. E. Barsoukov, J.R. Macdonald, *Impedance Spectroscopy: Theory, Experiment, and Applications (2nd ed.)*, Wiley Interscience, New York, 2005.

МОЖЕ ЛИ ФОРМАТЪТ НА ИНТЕРФЕЙСА ЕЛЕКТРОД/ЕЛЕКТРОЛИТ ДА ПРОМЕНИ ОБХВАТИТЕ НА ДИНАМИЧНИТЕ НЕСТАБИЛНОСТИ?

О.И. Гичан¹ и В.В.Потоцкая²

¹Чуйко институт по повърхностна химия към националната академия на науките на Украйна, 17 ул. Генерала Наумова 17, Киев 03164, Украйна

²Вернадски институт по обща и неорганична химия към националната академия на науките на Украйна, 32-34 Палладина Просп., Киев 03142, Украйна

Постъпила на 24 септември, 2014 г.; коригирана на 4 февруари, 2015 г.

(Резюме)

На базата на теорията на електрохимичната импедансна спектроскопия обхватите от динамични нестабилности водещи до осцилиращо и бистабилно поведение в модел на електрокаталитичен процес предшестван от химическа реакция в дифузионния слой на Нернст и потенциално зависимата адсорбция/десорбция на електроактивни видове при потенциостатични условия.